XL CILAMCE
IBERO-LATIN AMERICAN CONGRESS ON COMPUTATIONAL METHODS IN ENGINEERING
NOVEMBER 11-14, 2019
Praiamar Natal Hotel & Convention Natal, RN-BRAZIL

INVESTIGATION OF SOME PARAMETERS OF A LOW CONCENTRATION EVACUATED TUBE SOLAR COLLECTOR

Mavd R. Teles
Kamal A. R. Ismail
mavd.ribeiro@hotmail.com
kamal@fem.unicamp.br.com
State University of Campinas
Mendeleiev street, 200, Cidade Universitária "Zeferino Vaz", 13083-860, Barão Geraldo, Campinas - SP, Brazil

Abstract. This paper investigates the influence of essential parameters on a low concentration evacuated tube solar collector in their efficiency. The conventional models of evacuated tube solar collectors have an absorber tube covered by a glass tube with a vacuum between them. The studied model collector has an absorbing tube eccentrically positioned inside a glass cover tube which has a reflective film insert on its inner surface and vacuum in eccentric annular space. The proposed model is based on the conservation equations of mass, momentum and energy and discretized by using the finite volumes method. A home-built numerical code is developed to evaluate the desired parameters. This code is validated against available experimental and numerical results. The influence on the efficiency of parameters such as absorptivity of the absorber tube, reflectivity of the reflecting surface and radius of the absorber tube will be evaluated. Effects of the tracking systems in the thermal efficiency are also evaluated. The results showed that a 20% drop in the absorber's absorptivity can generate a 15% reduction in collector efficiency and a 10% drop in reflectivity of the reflecting surface can lead to a drop of around 4% in the efficiency of the solar collector.

Keywords: Solar energy, Evacuated tube solar collector; Eccentric evacuated tube collector

1 Introduction

The Paris agreement has established a commitment among countries to keep the global average temperature rise at well below 2 °C above pre-industrial levels. One of the sectors with the highest percentage of contribution to this goal is the energy sector. Due to its high availability, solar energy has a large share of contribution in the energy sector. The solar energy can be used to generate electric power, heat and also for cooling. According to Chopra et al. [1] among numerous applications of solar energy, water heating, space heating and cooling are consuming more energy and among all thermal collectors for low/medium temperature, the evacuated tube collector have the best efficiency. However, according to Sabiha et al. [2] there are still challenges and developments that need to be developed to make solar energy competitive, such as the efficiency of energy collected and storage.

The Paris agreement has established a commitment among countries to keep the global average temperature rise at well below 2 °C above pre-industrial levels. One of the sectors with the highest percentage of contribution to this goal is the energy sector. Due to its high availability, solar energy has a large share of contribution in the energy sector. The solar energy can be used to generate electric power, heat and also for cooling. According to Chopra et al. [1] among numerous applications of solar energy, water heating, space heating and cooling are consuming more energy and among all thermal collectors for low/medium temperature, the evacuated tube collector have the best efficiency. However, according to Sabiha et al. [2] there are still challenges and developments that need to be developed to make solar energy competitive, such as the efficiency of energy collected and storage.

A quick literature review shows that evacuated tube solar collectors received a lot of research attention which led to models and diversificated applications. For example, Singh et al. [3] in a solar still integrated with evacuated tube collector in natural mode and the variation of instant overall energy and exergy efficiencies found is the range of 5.1–54.4% and 0.15–8.25% respectively. Sharma and Diaz [4] investigated numerically the thermal performance of a solar collector based on minichannel. The minichannel-based collector generates an increase in heat transfer area between the absorber and the working fluid and the decrease in absorber resistance of the minichannel-based collector this generate an increase in efficiency in comparation with other collectors' models.

Mahbubul et al. [5] analyzed the effect of Single Walled Carbon Nanotube-water nanofluid on the efficiency of evacuated tubes solar collectors. Efficiency using water without addition of nanofluid showed a 56.7% efficiency result. Already using nanofluid 0.2 vol% for the same operating conditions resulted in an efficiency 66%. This result shows that the use of nanofluid can be very promising for enhance the efficiency of solar collectors.

A evacuated tube solar collector with multifunctional absorber layers and Phase Change Material (PCM) was developed by Sobhansarbandi et al. [6] to improve the efficiency. The addition of Carbon Nanotube sheets provide a near ideal black body surface, absorbing a maximum of 98% of solar light striking the surface. Applying PCM during the sunshine hours, the temperature remains around the constant value. During off sunshine hours, the PCM can delay the cooling rate of water by releasing stored latent heat energy, that can result in providing hot water to the demand side in cloudy days or when the solar radiation is insufficient.

Papadimitratos et al. [7] performed an experimental new method of integrate PCM in evacuated tube solar collectors. In this proposed solar collector, the heat pipe is immersed in the PCM. The benefit of this method includes improved functionality by delayed release of heat. The results from showed efficiency improvement of 26% and 66% for the stagnation mode, compared with standard solar water heaters.

Martínez-Rodríguez et al. [8] proposed a network of solar collectors as an association of heat transfer devices whose purpose is to deliver a working fluid at a specified temperature to meet a given heat load. This approach could be used at early design stages for assessing the cost benefit of the integration of solar energy into low energy intensity processes.

This study investigates the parameters on a low concentration evacuated tube solar collector. It will be developed a mathematical model to represent the physical phenomena and predict the thermal

performance of the collector. The solar collector is composed of an absorber tube set up eccentrically relative to the cover tube and between them exists vacuum. The underside of the cover tube has an internal reflective film responsible for the concentration of solar irradiation. The mathematical model is formulated based on the conservation equations (mass, momentum and energy) and discretized using the finite volume method. A numerical code is developed, tested and the numerical predictions are validated with available experimental results. The numerical code is used to investigate several parameters (absorptivity of the absorber, reflectivity of the reflective film and radius of the absorber) of the evacuated tube solar collector for the city of Campinas, Brazil. The results are presented and discussed.

2 Mathematical model

The model is composed of an external transparent tube that cover eccentrically the copper tube absorber, between them exists vacuum (Fig. 1). The cover tube has a reflective film on the internal surface of the bottom side. The reflective film reflects the incident solar radiation on the absorber tube. The eccentricity associated with the reflective film creates a concentrating effect of solar radiation at the absorber which increases the working temperature of the absorber of the collector. The presence of vacuum between the cover and the absorber helps reducing the radiation and convection losses. The absorber tube has a film on its surface to enhance absorbing solar radiation.

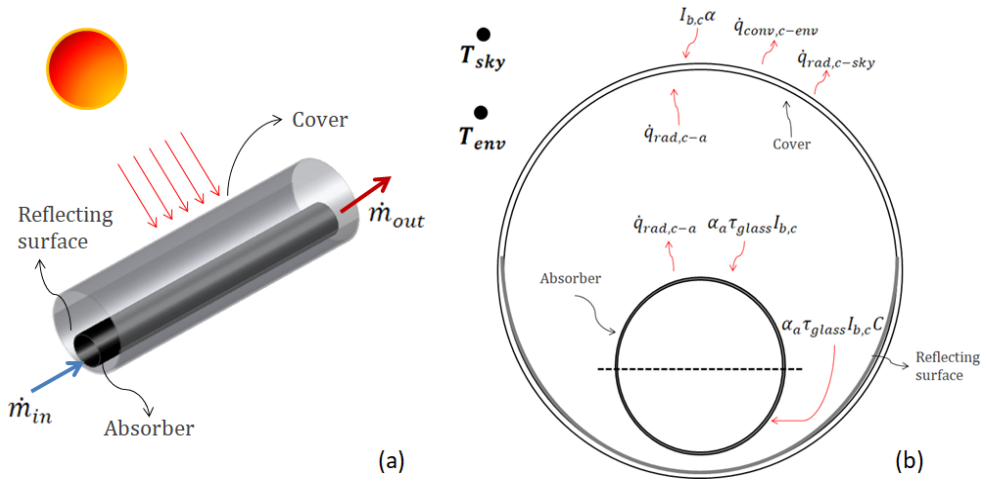

Figure 1. Scheme of the cover tube and absorber; (a) complete set; (b) collector cross-section showing the absorber and energy fluxes Teles et al. [9]

In Fig. 1 (b) the terms: $\dot{q}_{conv,c-env}$ refers to convection heat transfer between the transparent cover and the environment; $\dot{q}_{rad,c-sky}$ refers to radiation heat transfer between the transparent cover and the sky; $\dot{q}_{rad,c-a}$ refers to radiation between the cover and the absorber; $\alpha_a\tau_{glass}\, I_{b,c}$ refers to intercepted solar irradiation by the collector in a determined slope angle; $I_{b,c}\alpha$ refers to the solar irradiation absorbed by the cover and $\alpha_a\tau_{glass}\, I_{b,c}C$ refers to concentrated solar irradiation intercepted by the collector in a determined slope angle. The specifics variables are: α_a refers to the absorptivity of the absorber, $I_{b,c}$ solar irradiation intercepted by the collector plane, α refers to the absorptivity of the cover, τ_{glass} refers to the transmissivity of the glass cover and C refers to the concentration.

2.1 Parameters of the collector

The collector is composed of a glass cover, copper absorber and the working fluid is Therminol 66. All thermal properties of the different elements were obtained from Kreith et al. [10] and Solutia Europe S.A. [11], respectively. The tracking system of the collector is one axis following monthly the solar declination δ_s (annual cycle δ_s=±23.5° during the year) in approximate form. This type of

tracking utilizes the representative day of each month where the best declination angle is calculated and applied manually to the tracking mechanism instead of using automatic system which means additional cost. The collector orientation and the incidence angles were calculated for the city of Campinas, Brazil (Table 1) following Duffie and Beckman [12], Goswami et al. [13] and Teles et al. [9]. The negative values mean that the collector is facing the south while positive angles means facing the north.

Table 1. Collectors slope to the representative day of the month for the city of Campinas

Month	Jan.	Feb.	Mar.	Apr.	May	Jun.
Day	17	16	16	15	15	11
θ (°)	1.9	9.8	20.4	32.2	41.6	45.9
Month	Jul.	Aug.	Sep.	Oct.	Nov.	Dec.
Day	17	16	15	15	14	10
θ (°)	44	36.3	25	13.2	3.9	-0.2

The dimensions of the solar collector are shown in Table 2, where the specific variables are: $R_{c,ext}$ refers to the external cover's radius, $R_{c,int}$ refers to the internal cover's radius, $r_{a,ext}$ refers to the external absorber's radius, $r_{a,int}$ refers to the internal absorber's radius and L_c refers to the length of the collector.

Table 2. Parameters of the model of the solar collector

$R_{c,ext}$ (m)	$R_{c,int}$ (m)	$r_{a,ext}$ (m)	$r_{a,int}$ (m)	L_c (m)	Concentration ratio (C)
0.05	0.0484	0.024	0.0224	1.8	2.083

2.2 Formulation and Numerical treatment

The developed mathematical is based on the conservation equations in permanent regime of mass, momentum and energy. The thermo-physical properties of the constructive materials of the collector and the working fluid are assumed independent of the temperature except for the fluid density and viscosity which are allowed to vary with temperature. The collector and tubes extremities (entry and exit of the working fluid) are considered adiabatic. The fluid flow regime is considered laminar and the fluctuation forces are calculated from Boussinesq´s approximation. Considering the hypotheses, the conservation equations for the domain:

Continuity:

$$\frac{\partial(\rho u)}{\partial x} + \frac{\partial(\rho v)}{\partial r} = 0. \tag{1}$$

Momentum:

$$u\frac{\partial(\rho u)}{\partial x} + v\frac{\partial(\rho u)}{\partial r} = -\frac{\partial P}{\partial x} + \mu\left(\frac{\partial^2 u}{\partial x^2} + + \frac{1\partial}{r\partial r}\left(r\frac{\partial u}{\partial r}\right)\right) + (\rho_{ref} - \rho)g\,sin(\theta). \tag{2}$$

$$u\frac{\partial(\rho v)}{\partial x} + v\frac{\partial(\rho v)}{\partial r} = -\frac{\partial P}{\partial r} + \mu\left(\frac{\partial^2 v}{\partial x^2} - \frac{v}{r^2} + \frac{1\partial}{r\partial r}\left(r\frac{\partial v}{\partial r}\right)\right) + (\rho_{ref} - \rho)g\,cos(\theta). \tag{3}$$

Energy:

$$u\frac{\partial(\rho T)}{\partial x} + v\frac{\partial(\rho T)}{\partial r} = \frac{k}{cp}\left(\frac{\partial^2 T}{\partial^2 x} + \frac{1\partial}{r\partial r}\left(r\frac{\partial T}{\partial r}\right)\right) + \frac{S}{cp}. \tag{4}$$

The variables are: ρ refers to density (kg/m³), u refers to the velocity in x-axis (m/s), v refers to the velocity in r-axis (m/s), P refers to the pressure (Pa), μ refers to the dynamic viscosity N s/m², ρ_{ref} refers to density of reference, g refers to the gravity (m/s²), T refers to the temperature (K), k refers to thermal conductivity (W/mK), cp refers to the specific heat (J/kg K) and S is the source term.

The general equation for steady-state regime that represents all conservation equations according to Patankar [14] can be expressed as:

$$\vec{\nabla}\left(\rho\vec{V}\emptyset\right) = \vec{\nabla}\left(\Gamma\vec{\nabla}\emptyset\right) + S. \tag{5}$$

The variables are: $\vec{\nabla}$ refers to divergent, $\vec{V}$ refers to the vector velocity, $\emptyset$ refers to the generic extensive property and Γ refers to the diffusive coefficient.

The fluxes of energy incident and reflected from the collector elements are shown in Fig. 1 and are the same as used by Teles et al. [9]. The equations which define the boundary conditions in the North (M) and in the south (1) of the glass cover are, respectively:

$$-\left(k\frac{\partial T}{\partial r}\right)_M = \alpha_{glass} I_{b,c} + \varepsilon\sigma\left(T_{sky}^4 - T_M^4\right) + h_{conv,c-sky}(T_{env} - T_M). \tag{6}$$

$$-\left(k\frac{\partial T}{\partial r}\right)_1 = F_{2-1}\varepsilon\sigma\left(T_{absorber}^4 - T_1^4\right). \tag{7}$$

The variables are: ε refers to emissivity, σ refers to the Stefan-Boltzmann constant [W/(m²K⁴)], T_{env} refers to the environment temperature, h refers to the heat transfer coefficient [W/(m²K)] and F refers to the shape factor.

The boundary conditions of the glass cover for the West (1) and east (N) are respectively:

$$T(N, r) = T(N-1, r). \tag{8}$$

$$T(1, r) = T(2, r). \tag{9}$$

The absorber according to Fig. 1 has one half is subject to concentration effect while the upper half does not receive any concentration effect. Hence there are two north boundary conditions represented by the equations:

$$-\left(k\frac{\partial T}{\partial r}\right)_M = C\alpha_a\tau_{glass} I_{b,c} + F_{2-1}\varepsilon\sigma(T_{cover}^4 - T_M^4). \tag{10}$$

$$-\left(k\frac{\partial T}{\partial r}\right)_M = \alpha_a\tau_{glass} I_{b,c} + F_{2-1}\varepsilon\sigma(T_{cover}^4 - T_M^4). \tag{11}$$

The south of the absorber is considered adiabatic because of the symmetry, and the equations which represent the boundary conditions in the south, east and west are:

$$T(x, 1) = T(x, 2). \tag{12}$$

$$T(N, r) = T(N-1, r). \tag{13}$$

$$T(1, r) = T(2, r). \tag{14}$$

The initial conditions, the fluid and other elements were considered initially at ambient temperature. The initial fluid velocity is equal to $u_{initial} = 0.005$ (m/s), while in the solid region u=v=0. All properties and empirical coefficients were adopted from Teles et al. [9].

The equations of the mathematical model and the associated boundary and initial conditions are treated numerically by using the method of finite volumes in the axial and radial directions for the different segments of the proposed evacuated tube collector. The segments include the glass cover and the absorber with and without concentration of the solar irradiation as in Teles et al. [9]. The power law is the discretization scheme used for the convective and diffusive terms. The numerical code is written in FORTRAN and the algorithm SIMPLE was used to couple the pressure and velocity. The TDMA line-by-line (Tri-Diagonal Matrix Algorithm) method was used to solve the equations. The chosen computational grid is uniform and the solid fluid interface coincide with the faces of the control volume. The iteration process starts at an arbitrary time and the convergence criterion is satisfied by Eq. (14).

$$\sum_{i,j}\left|\frac{\emptyset_{ij}^{n}-\emptyset_{ij}^{n+1}}{\emptyset_{ij}^{n}}\right| \leq \xi. \tag{14}$$

Where ∅ can be the variables u, v, T or P. The index n is the iteration order and the value of ξ chosen as 10^{-6}.

A fair number of tests were done to select the optimum grid and the most suitable grid is found to be 22x13 for the absorber.

2.3 Validation

The experimental results of Kim et al. [15] were used to validate the present numerical model since both collectors have low concentration ratio and eccentric absorber tube with direct fluid flow, but the collector simulated by Kim et al. [15] had a second glass cover. Fig. 2 shows the cross sections of the two collectors and the heat and radiation fluxes.

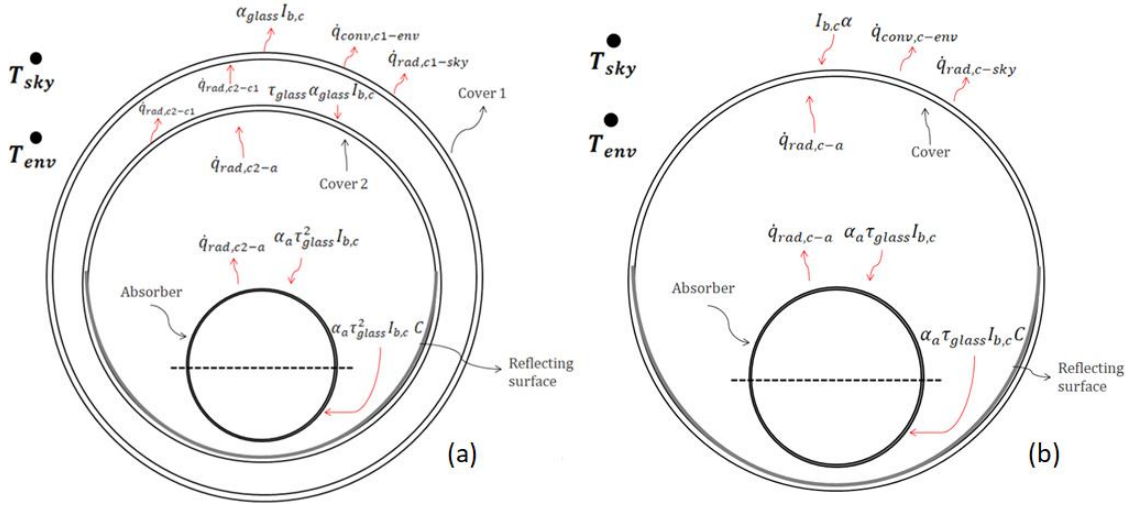

Figure 2. Collectors cross-section with the absorber and the specified boundary conditions (a) reference collector, (b) present model Teles et al. [9]

Figure 3 shows a comparison between the present predicted heat flux and collector outlet temperature with those obtained from Kim et al. [15] showing relatively good agreement with error of about 0.36% for the temperature and about 2% for the heat flux.

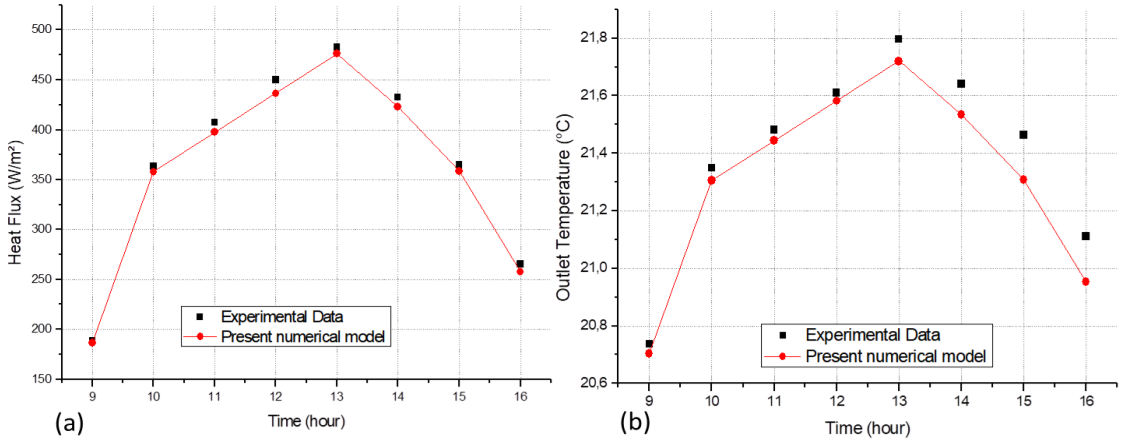

Figure 3. Comparison of the heat flux and the fluid outlet temperatures from the present predictions with the results from Kim et al. [15]

3 Results and discussion

The simulations conducted for the representative day of December in the period from 9h to 16 h, are presented in Table 1 for the city of Campinas. The simulations were done to test the one-axis tracking system (declination cycle ± 23.5°). Evaluation included the effects on the efficiency of the absorber diameter, absorptivity of the film and reflectivity of the reflecting surface.

3.1 Degradation's effects of the reflective film

The reflecting surface is placed in the internal part of the cover and is responsible for part of the solar irradiation on the absorber's collector. Hence, the degradation of the surface reflectivity (ρ_0) directly impacts the efficiency of the solar collector. Fig. 4 shows simulation results for the hourly efficiency for different values of reflectivity.

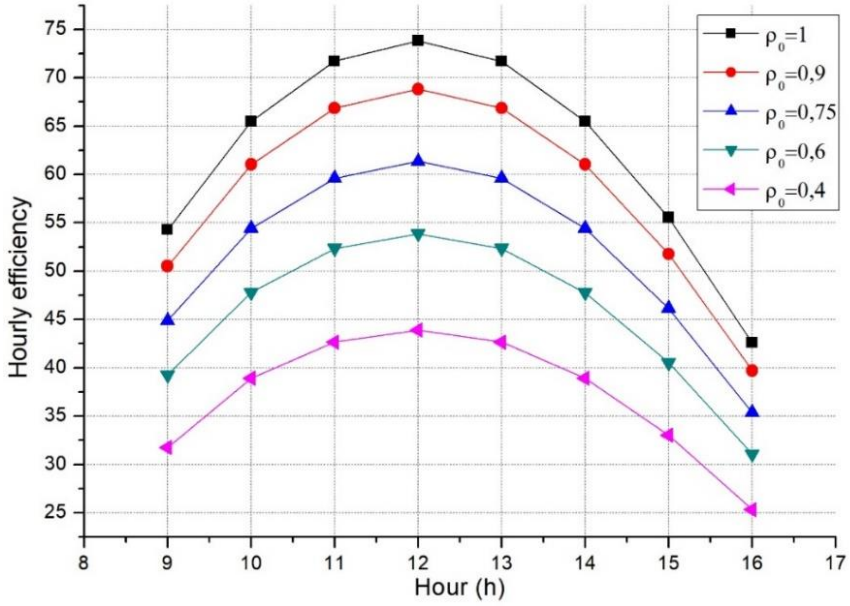

Figure 4. Hourly efficiency for different values of the reflective film

The degradation of the reflectivity significantly reduces the collector efficiency, a difference of $\Delta\rho_0 = 0.4$ causes a reduction of 19% in the collector efficiency. This analysis also allows to measure other aspects of low concentration ratio. Different models of concentrating collectors have low efficiency because they don't have small concentration. Kim and Seo [16] evaluated different models of evacuated tube solar collectors and concluded some of these collectors without concentration showed maximum efficiency of about 65%.

3.2 Degradation's effects of the absorber film

The degradation of the absorptivity of the absorbing film reduce the collector efficiency. Simulations of the hourly efficiency for various values of film absorbance are shown in Fig. 5. As one can observe the influence of the absorptivity of the film is stronger on the reduction of the hourly efficiency than the reflectivity of the reflecting surface. A reduction of $\Delta\alpha = 0.4$ reduce the collector efficiency by about 28%. Hence it is imperative to choose a film with high absorptivity to ensure high thermal performance of the collector.

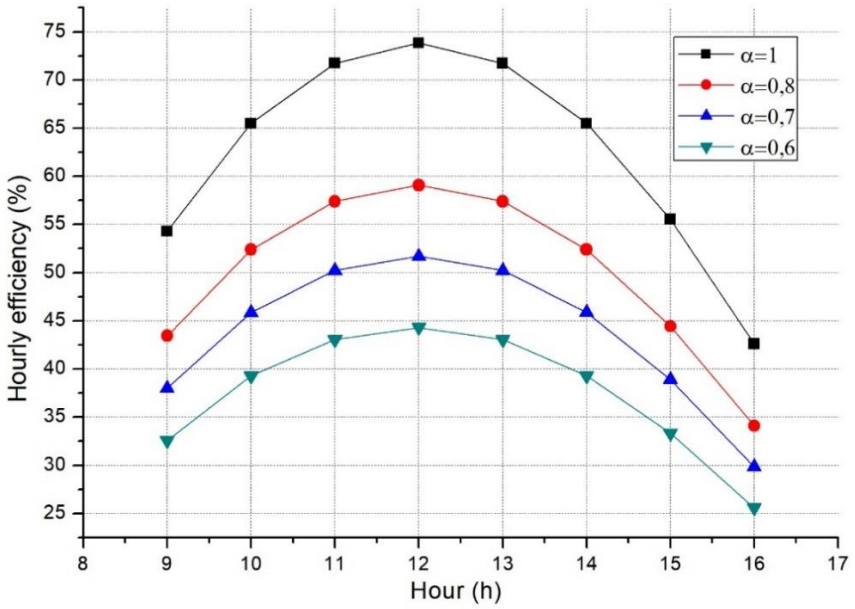

Figure 5. Hourly efficiency for different values of the absorptivity of the absorber film

3.3 Effect of the absorber diameter

To illustrate the effect of the diameter of the absorber tube on the efficiency of the collector simulations were done for three tube diameters keeping other variables unchanged as the mass flow rate of the working fluid. Few simulations were done varying the absorber's diameter for 0.048, 0.044, and 0.040m, while keeping the radius of the cover as $R_{c,ext} = 0.05$ m, as shown in Fig. 6.

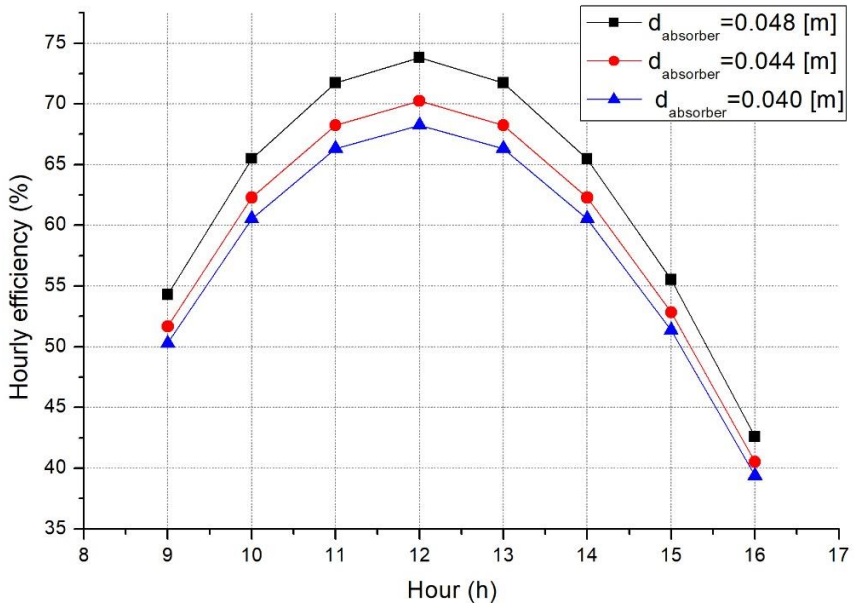

Figure 6. Hourly efficiency for different values of the absorber radius

As can be seen, reducing the absorber diameter reduce the hourly efficiency of the collector by about 2%. The reduction of the absorber diameter while keeping the flow rate of the working fluid constant increases the surface temperature of the absorber. This increases radiation to the covering cover and external ambient and consequently increases the thermal losses.

Also increasing the diameter of the absorber while keeping the mass flow rate constant decreases the Reynolds number and consequently the internal heat transfer coefficient which leads to lower heat

gain and lower surface temperature which favors less energy loss and hence better efficiency.

4 Conclusions

This paper reports the results of a numerical study to investigate the effects of the variation of the absorptivity of the absorber, reflectivity of the reflective surface and diameter of the absorber on the hourly efficiency of the evacuated tube eccentric solar collector. The numerical code based on the developed model was optimized and validated against available experimental results showing good agreement with error of 2% in the heat flux and 0.36% in the outlet temperature of the working fluid.

Simulations were performed to investigate the effects of the degradation of the reflectivity of the reflective film, degradation of the absorptivity of the absorber tube and effect of the diameter of the absorber on the hourly efficiency of the collector.

Degradation of the reflectivity of the film can reduce significantly the hourly efficiency of the solar collector. A reduction of $\Delta\rho_0 = 0.4$ is found to reduce the efficiency of the collector by 19%. This means it is important to replace the film when achieving this poor performance.

Degradation of the absorptivity of the absorber impairs significantly the thermal performance of the collector. It is found that a decrease of $\Delta\alpha = 0.4$ reduces the hourly efficiency by 28%.

The effect of the diameter of the absorber is of great significator collectors with internal concentration as the proposed collector. For the investigated absorber diameters, a reduction of about 2% in the hourly efficiency is observed.

Acknowledgements

The authors wish to thank the Fundação de Amparo à Pesquisa e ao Desenvolvimento Científico e Tecnológico do Maranhão (Fapema) for the doctorate grant [grant number BD-08373/17] and the second author wishes to thank the Conselho Nacional de Desenvolvimento Científico e Tecnológico (CNPq) for the PQ Research Grant 304372/2016-1.

References

[1] K. Chopra; V. V. Tyagi; A. K. Pandey and A. Sari. Global advancement on experimental and thermal analysis of evacuated tube collector with and without heat pipe systems and possible applications. *Applied Energy*, vol. 228, pp. 351–389, 2018.

[2] M. A. Sabiha; R. Saidur; S. Mekhilef and O. Mahian. Progress and latest developments of evacuated tube solar collectors. *Renewable and Sustainable Energy Reviews*, vol. 51, pp. 1038–1054, 2015.

[3] R. V. Singh; S. Kumar; M. M. Hasan; M. E. Khan and G. N. Tiwari. Performance of a solar still integrated with evacuated tube collector in natural mode. *Desalination*, vol. 318, pp. 25–33, 2013.

[4] N. Sharma and G. Diaz. Performance model of a novel evacuated-tube solar collector based on minichannels. *Solar Energy*, vol. 85, n. 5, pp. 881–890, 2011.

[5] I. M. Mahbubul; M. M. A. Khan; N. I. Ibrahim; H. M. Ali; F. A. Al-Sulaiman and R. Saidur. Carbon nanotube nanofluid in enhancing the efficiency of evacuated tube solar collector. *Renewable Energy*, vol. 121, pp. 36–44, 2018.

[6] S. Sobhansarband; P. M. Martinez; A. Papadimitratos and A. Zakhidov. Evacuated tube solar collector with multifunctional absorber layers. *Solar Energy*, vol. 146, pp. 342–350, 2017.

[7] A. Papadimitratos; S. Sobhansarbandi; V. Pozdin; A. Zakhidov and F. Hassanipour. Evacuated tube solar collectors integrated with phase change materials. *Solar Energy*, vol. 129, pp. 10–19, 2016.

[8] G. Martínez-Rodríguez; A. L. Fuentes-Silva and M. Picón-Núñez. Solar thermal networks operating with evacuated-tube collectors. *Energy*, vol. 146, pp. 26–33, 2018.

[9] M. R. Teles; K. A. R. Ismail and A. Arabkoohsar. A new version of a low concentration evacuated tube solar collector: Optical and thermal investigation. *Solar Energy*, vol. 180, pp. 324–339, 2019.

[10] F. Kreith; R. Manglik and M. Bohn. *Principles of heat transfer*. Cengage Learning, 2011.
[11] Solutia Europe S.A. Therminol 66 Thermal Properties. Disponível em: <http://twt.mpei.ac.ru/TTHB/HEDH/HTF-66.PDF>. Accessed in: 1 may. 2018.
[12] J. A. Duffie and W. A. Beckman. *Solar engineering of thermal processes*. John Wiley & Sons, 2013.
[13] D. Y. Goswami; F. Kreith and J. Kreider. *Principles of solar engineering*. Taylor & Francis, 2000.
[14] S. V. Patankar. *Numerical heat transfer and fluid flow*. Hemisphere Pub. Corp., 1980.
[15] Y. Kim; G. Y. Han and T. Seo. An evaluation on thermal performance of CPC solar collector. *International Communications in Heat and Mass Transfer*, vol. 35, n. 4, pp. 446–457, 2008.
[16] Y. Kim and T. Seo. Thermal performances comparisons of the glass evacuated tube solar collectors with shapes of absorber tube. *Renewable Energy*, vol. 32, n. 5, pp. 772–795, 2007.
[17] M. R. Teles; R. Carvalho and K. Ismail. Optical analysis of low concentration evacuated tube solar collector. *Advances in Energy Research*, vol. 5, pp. 227–237, 2017.